The Plant Cell, Vol. 22: 904–917, March 2010, www.plantcell.org

High-Affinity Manganese Uptake by the Metal Transporter NRAMP1 Is Essential for *Arabidopsis* Growth in Low Manganese Conditions [W]

Rémy Cailliatte, Adam Schikora,[1] Jean-François Briat, Stéphane Mari, and Catherine Curie[2]

Laboratoire de Biochimie et Physiologie Moléculaire des Plantes, Centre National de la Recherche Scientifique, Unité Mixte de Recherche 5004, Institut de Biologie Intégrative des Plantes, F-34730 Montpellier cedex 2, France

In contrast with many other essential metals, the mechanisms of Mn acquisition in higher eukaryotes are seldom studied and poorly understood. We show here that *Arabidopsis thaliana* relies on a high-affinity uptake system to acquire Mn from the soil in conditions of low Mn availability and that this activity is catalyzed by the divalent metal transporter NRAMP1 (for Natural Resistance Associated Macrophage Protein 1). The *nramp1-1* loss-of-function mutant grows poorly, contains less Mn than the wild type, and fails to take up Mn in conditions of Mn limitation, thus demonstrating that NRAMP1 is the major high-affinity Mn transporter in *Arabidopsis*. Based on confocal microscopy observation of an NRAMP1-green fluorescent protein fusion, we established that NRAMP1 is localized to the plasma membrane. Consistent with its function in Mn acquisition from the soil, *NRAMP1* expression is restricted to the root and stimulated by Mn deficiency. Finally, we show that NRAMP1 restores the capacity of the *iron-regulated transporter1* mutant to take up iron and cobalt, indicating that NRAMP1 has a broad selectivity in vivo. The role of transporters of the NRAMP family is well established in higher eukaryotes for iron but has been controversial for Mn. This study demonstrates that NRAMP1 is a physiological manganese transporter in *Arabidopsis*.

INTRODUCTION

All organisms require trace levels of Mn for survival. Mn is a transition metal that can exist in several different valence states and therefore plays the role of catalyst in electron transfer reactions when used as a protein cofactor. Mn is a constituent of essential metalloenzymes, including the antioxidant defense enzyme Mn^{2+}-dependent superoxide dismutase (Marschner, 1995) and, in photosynthetic organisms, the four Mn atom-containing oxygen evolving complex that catalyzes water oxidation in photosystem II (Merchant and Sawaya, 2005). In addition, Mn is an activator of numerous enzymes involved in diverse metabolic pathways, such as DNA synthesis, sugar metabolism, or protein modification. Except for glycosyltransferases, however, many of these enzymes are nonspecific and can use Mg^{2+} as a replacement for Mn^{2+} (Crowley et al., 2000).

Like all essential transition metals, Mn in excess can be harmful. Because Mn and Fe compete for common transporters and ligands, the classical effect of dietary Mn toxicity is a secondary Fe deficiency. In animals, Mn toxicity often occurs by chronic inhalation of Mn oxides and results in neurological damages (Keen et al., 2000). In plants, high concentrations of Mn cause chlorosis, brown speckles on mature leaves, and necrosis, which result in reduced crop yield (Marschner, 1995).

Mn deficiency is rarely observed due to the low requirement for Mn in cells. Mn deficiency symptoms in animals include defects in lipid, carbohydrate, and protein metabolism, leading to reduced growth and skeletal abnormalities (Keen et al., 2000). In plants, Mn deficiency occurs in calcareous soils or alkaline soils that favor Mn oxidation and immobilization of Mn^{2+}. In addition, when iron occurs in excess in the culture medium, it can compete with Mn and trigger a Mn deficiency. Mn deficiency symptoms are denoted by a yellowing of the young leaves in dicotyledonous plants or the development of gray specks in the mature leaves of cereals (Marschner, 1995). In addition, the patterning and development of root hairs is altered in Mn-deficient *Arabidopsis thaliana* (Yang et al., 2008). The metabolic impact of Mn deficiency has been little investigated compared with Fe deficiency, although, recently, the molecular consequences of Mn deficiency have been studied in *Chlamydomonas reinhardtii* (Allen et al., 2007). In this organism, Mn-deficient cells have compromised photosystem II function, reduced MnSOD activity, and are sensitive to peroxide stress. Mn deficiency in *Chlamydomonas* results in (1) secondary Fe deficiency and (2) decrease of the cell phosphorus content, probably owing to the phosphorus PHO84-like transporters that use Mn^{2+} as preferred counterion (Jensen et al., 2003). Contrary to *Chlamydomonas*, Mn-deficient roots of *Arabidopsis* have an elevated Fe concentration, decreased expression of Fe deficiency–induced genes, and increased expression of ferritin genes (Yang et al., 2008). This discrepancy

[1] Current address: Institute for Phytopathology and Applied Zoology, Justus-Liebig University Giessen, Heinrich-Buff-Ring 26-32, D-35392 Giessen, Germany.
[2] Address correspondence to curie@supagro.inra.fr.
The author responsible for distribution of materials integral to the findings presented in this article in accordance with the policy described in the Instructions for Authors (www.plantcell.org) is: Catherine Curie (curie@supagro.inra.fr).
[W] Online version contains Web-only data.
www.plantcell.org/cgi/doi/10.1105/tpc.109.073023

may reflect the difference of response to oxidative stress between these two organisms.

Several proteins that may transport Mn have been identified in plants, such as members of the CAX, CDF, or P2A-type ATPase families, but they are all involved in intracellular Mn traffic (Maser et al., 2001; Hall and Williams, 2003; Delhaize et al., 2007; Peiter et al., 2007; Li et al., 2008; Mills et al., 2008). By contrast, little is known about Mn uptake from the environment and about the kinetics of this transport in plants (Pittman, 2005), whereas knowledge has increased tremendously for most nutrients in recent years. The demonstration of the presence of a high-affinity Mn^{2+} uptake system, showing an apparent K_m value of 0.3 μM and a low specificity (Gadd and Laurence, 1996), was first provided in yeast *Saccharomyces cerevisiae*. In plants, similar results were absent until recently because of the difficulty in monitoring Mn uptake in realistically low concentrations of Mn. Recently, the existence of two separate Mn transport systems mediating high-affinity and low-affinity uptake of Mn^{2+} was elegantly shown in winter barley (*Hordeum vulgare*; Pedas et al., 2005). The iron-regulated transporter IRT1 represents a putative pathway for entry of Mn into the cell. IRT1 is the major high-affinity transporter for Fe^{2+} acquisition in iron-limited conditions but also transports a range of metal ions, including Mn^{2+} (Eide et al., 1996; Korshunova et al., 1999; Vert et al., 2002). Analysis of a knockout mutant indicated that IRT1 accounts for most of the Mn entry into the roots of Fe-deficient plants, even although the drastic chlorotic phenotype of the *irt1-1* mutant can be rescued only by supplying Fe and not Mn (Vert et al., 2002). The expression of barley *IRT1* was shown to be 40% greater in a Mn-efficient genotype (Pedas et al., 2008), suggesting that IRT1 may contribute to Mn acquisition in this species.

The evolutionarily conserved transporter family NRAMP/Divalent Cation Transporter 1/Divalent Metal Transporter 1 (DCT1/DMT1) has been shown to play a major role in metal homeostasis in species ranging from bacteria to man (Nevo and Nelson, 2006). These proteins are proton/metal symporters that have a broad spectrum of metal cation substrates, including Fe^{2+}, Mn^{2+}, Zn^{2+}, Cd^{2+}, Co^{2+}, Cu^{2+}, Ni^{2+}, and Pb^{2+} (Gunshin et al., 1997; Nevo and Nelson, 2006). A disruption of mammalian NRAMP2, as in microcytic mouse or Belgrade rat, causes anemia (Fleming et al., 1997, 1998). NRAMP2 is located at the brush border of enterocyte cells as well as in peripheral tissues where it takes up Fe and presumably Mn. NRAMP1, the other member of the family in mammals, is required for macrophage defense against pathogens, probably by reducing the concentration of metals in the pathogen-containing phagosomes and thereby limiting pathogen propagation (Vidal et al., 1993; Nevo and Nelson, 2006). Mn uptake by bacteria occurs via the H^+-coupled Mn transporter MntH, an NRAMP homolog (Kehres et al., 2000; Makui et al., 2000). MntH has preferential affinity for Mn^{2+}, but can also take up Fe^{2+}. In *Saccharomyces cerevisiae*, two of the three NRAMP members, Smf1p and Smf2p, act sequentially in the uptake and trafficking of Mn (Portnoy et al., 2000). Both proteins are required to maintain Mn levels constant under conditions of Mn deprivation. Smf1p and Smf2p are regulated posttranslationally by Mn starvation, which enhances protein stability as well as shifts cellular localization of the proteins to their target membranes (Liu and Culotta, 1999; Jensen et al., 2009).

Transporters of the NRAMP family have been identified in many plant species (Belouchi et al., 1995, 1997; Curie et al., 2000; Thomine et al., 2000; Bereczky et al., 2003; Kaiser et al., 2003; Mizuno et al., 2005; Xiao et al., 2008; Oomen et al., 2009; Wei et al., 2009). Five of the six *Arabidopsis NRAMP* genes have been characterized at the molecular level, *NRAMP1-4* and *6* (Curie et al., 2000; Thomine et al., 2000; Cailliatte et al., 2009). So far, however, only NRAMP3 and NRAMP4 have been assigned a biological function. Both proteins are located on the vacuolar membrane in the embryo where they mediate the mobilization of vacuolar iron stores to support early plant development (Lanquar et al., 2005). In this study, we establish that NRAMP1 functions as a physiological Mn transporter in *Arabidopsis* and that it is required for high-affinity Mn uptake into the root in conditions of low Mn availability.

RESULTS

Knocking Out *NRAMP1* Results in Hypersensitivity to Mn Deficiency

In a previous work, we showed that transgenic *Arabidopsis* lines overexpressing *NRAMP1* are more tolerant to iron toxicity, suggesting a role for NRAMP1 in iron homeostasis (Curie et al., 2000). To directly address the physiological function of NRAMP1, we characterized an *Arabidopsis* T-DNA insertional mutant, named *nramp1-1*, from the SALK collection (SALK_053236). In the *nramp1-1* allele, the T-DNA is inserted in the ninth exon of the *NRAMP1* gene. The *NRAMP1* transcript was not detectable in this line, as shown by RT-PCR (Figure 1A), indicating that *nramp1-1* is a null allele of *NRAMP1*. We found no apparent phenotype of the *nramp1-1* mutant when grown in the presence of various concentrations of iron. Since *NRAMP1* is able to rescue the Mn uptake defect of *smf1* yeast strain (Thomine et al., 2000), we investigated *nramp1-1* behavior in response to Mn availability. When cultivated in vitro in a medium lacking Mn, *nramp1-1* plants were paler (Figure 1B), produced 2.5-fold less biomass (Figure 1C), and showed a root growth rate up to twofold lower (Figure 1D) than wild-type plants. In the presence of an excess of Mn (750 μM) in the medium, however, the observed growth inhibition was indistinguishable between wild-type and mutant plants (Figures 1B and 1C), thus ruling out the possibility that knocking out *NRAMP1* would increase the plant tolerance to Mn toxicity.

Mn Accumulation Is Impaired in *nramp1-1*

To test whether the poor growth of *nramp1-1* in limited Mn availability is a consequence of an alteration of the plant Mn content, we measured metal content by inductively coupled plasma–mass spectrometry (ICP-MS) in shoots and roots of wild-type and *nramp1-1* plants cultivated in vitro in either Mn-replete (20 μM) or Mn-deficient (no Mn) medium during 2 weeks (Figure 2). As expected, we observed a drastic reduction (more than threefold) in the concentration of Mn in the shoots of *nramp1-1* plants grown under Mn deficiency (Figure 2A). The concentration of Mn in the roots, however, was not significantly

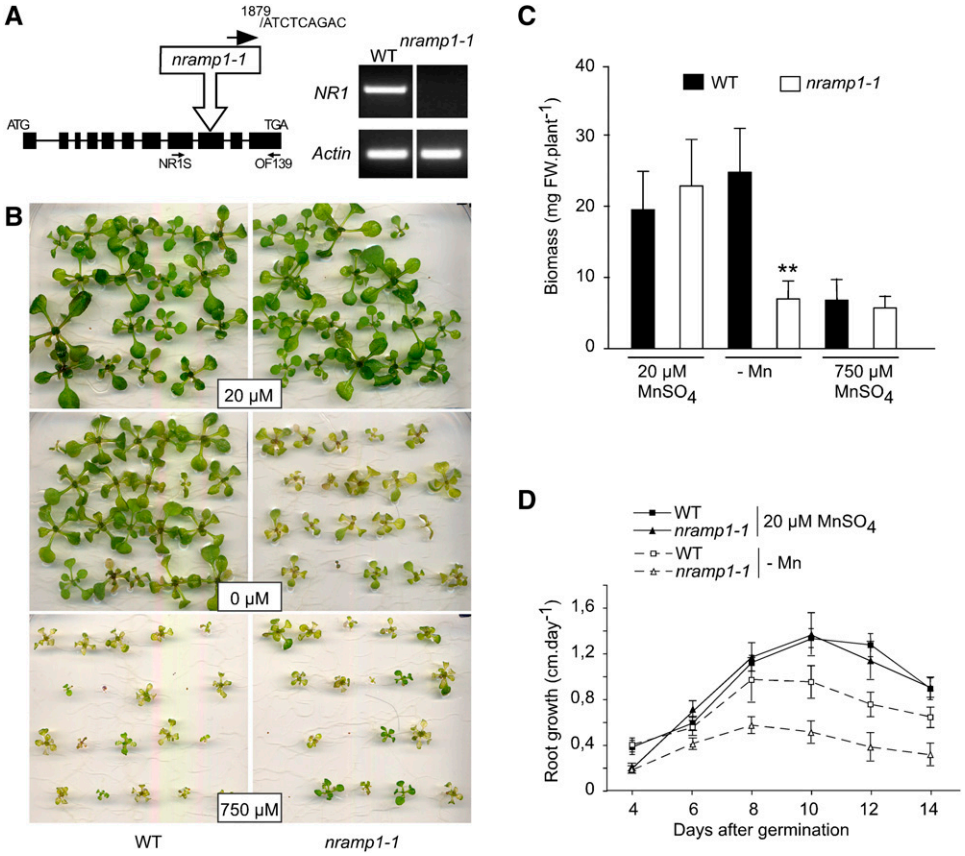

Figure 1. The *nramp1-1* Knockout Allele of *NRAMP1* Is Hypersensitive to Mn Deficiency.

(A) The *nramp1-1* mutant contains a T-DNA inserted in the 9th exon of the *NRAMP1* gene and results in complete loss of accumulation of *NRAMP1* mRNA as shown by RT-PCR.

(B) Test of tolerance to Mn deficiency of wild-type and *nramp1-1* plants grown in vitro for 14 d either in Mn-replete conditions (20 μM $MnSO_4$), in Mn-free medium (no added Mn), or in Mn excess medium (750 μM $MnSO_4$) as indicated.

(C) Biomass production of plants grown as in **(B)**. Data are from one representative experiment ($n = 2$). Error bars represent SD. **, Significant difference between the wild type and *nramp1-1*, $P < 0.001$, $n = 8$ (Student's *t* test). FW, fresh weight.

(D) Root elongation rate of wild-type and *nramp1-1* plants grown in vitro in either Mn-replete (+Mn, 20 μM $MnSO_4$) or Mn-free (−Mn, no added Mn) medium. Values are the means of 20 plants. Data are from one representative experiment ($n = 2$). Error bars represent SD.

decreased in the mutant (Figure 2A). In Mn-replete conditions, Mn content was identical in shoots of wild-type and mutant plants, consistent with the lack of a macroscopic phenotype of the *nramp1-1* mutant in these growth conditions (Figure 2B). Nevertheless, roots of the mutant contained twofold less Mn than wild-type roots, even though no growth defect was detected in these conditions (Figures 1B to 1D). Because iron was shown by heterologous expression in yeast to be a substrate of NRAMP1, we tested whether Fe content was also affected in the *nramp1-1* mutant. Regardless of the Mn concentration in the medium, Fe content remained essentially unaffected by the mutation (Figures 2C and 2D). Likewise, the amount of Zn or Cu was not modified in the mutant (Table 1). Cobalt concentration, however, decreased by 40% both in roots of Mn-replete *nramp1-1* plants and in shoots of Mn-deficient plants, thus following the same trend as Mn (Table 1). Altogether, these results confirm that accumulation of Mn, and to a lesser extent accumulation of Co, is altered in the *nramp1-1* mutant, a result that is consistent with the growth defect observed under Mn-limited conditions.

Overexpression of *NRAMP1* Rescues the *nramp1-1* Phenotype and Increases Tolerance to Mn Deficiency

To perform a complementation test, the *nramp1-1* line was transformed with a construct containing NRAMP1 fused to green fluorescent protein (GFP) under the control of the cauliflower mosaic virus (CaMV) *35S* promoter. Production of the NRAMP1-GFP protein in the *nramp1-1* mutant was tested by immunoblot analysis on root proteins probed with anti-GFP antibodies. Among transgenic lines #4, 6, and 9 that presented a strong GFP signal in immunoblot analysis (Figure 3A), line #4 was grown hydroponically for 4 weeks under Mn-replete or -deficient conditions together with wild-type and *nramp1-1* untransformed mutant plants. In replete conditions, no growth difference was

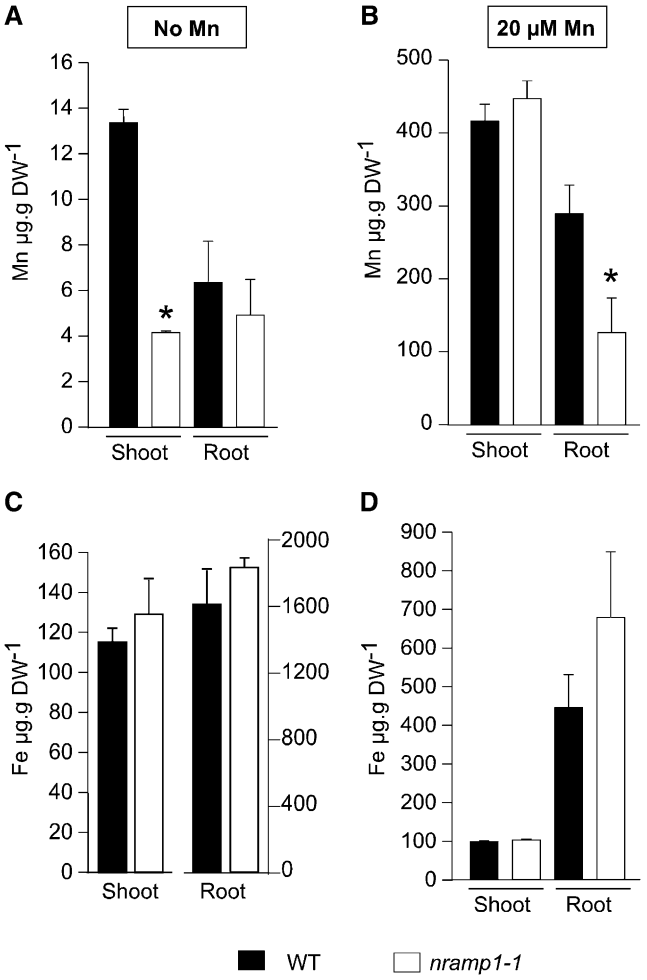

Figure 2. Mn Concentration Is Altered in the *nramp1-1* Mutant.

Elemental analysis was performed by ICP-MS on roots and shoots of wild-type or *nramp1-1* plants grown for 2 weeks in vitro either in Mn-replete (20 µM $MnSO_4$) or in Mn-free (no added Mn) medium as indicated in the figure. Data are from one representative experiment ($n = 2$). Error bars represent SD. *, Significant difference between the wild type and *nramp1-1*, $P < 0.01$, $n = 5$ (Student's *t* test). DW, dry weight.

(A) and **(B)** Mn content.

(C) and **(D)** Fe content.

observed between the plants. In the absence of added Mn, however, the phenotypic defect of *nramp1-1* was clearly rescued by NRAMP1-GFP, as shown for complemented line #4 in terms of both shoot growth (Figure 3B) and root biomass production (Figure 3C). Furthermore, NRAMP1-GFP restored Mn content in the *nramp1-1* mutant (Figure 3D). This result confirmed that *nramp1-1* phenotypic disorders are caused by the loss of NRAMP1.

In addition to complementing *nramp1-1* phenotype, the overexpression of NRAMP1-GFP provoked a hypertolerance of the plants to Mn deficiency, as shown by the size of these plants and their Mn content, both of which exceeded that of wild-type plants (Figures 3B to 3D). The finding that plants containing more of the NRAMP1 transporter are more tolerant to Mn deficiency is in good agreement with the loss of tolerance to Mn deficiency of the *nramp1-1* mutant and further argues in favor of the role of NRAMP1 in improving Mn availability to plants in Mn limiting conditions.

NRAMP1 Expression Is Restricted to the Root and Upregulated by Mn Deficiency

The level of expression of *NRAMP1* was determined by real-time RT-PCR in the root and shoot of plants grown for 3 weeks in hydroponic culture. We found *NRAMP1* transcripts to be 10 times more abundant in roots than in shoots (Figure 4A). In addition, the level of transcripts increased 2.5-fold when plants were grown in the absence of Mn (Figure 4A). We next analyzed the kinetics of response of *NRAMP1* to Mn deficiency and resupply. Ten-day-old plants grown in vitro in Mn-replete conditions were transferred to Mn-deficient medium, and *NRAMP1* transcript abundance was measured over time by real-time quantitative RT-PCR. After an initial decline in expression level, *NRAMP1* transcript abundance slowly increased after 5 d of Mn deficiency to reach its maximal level at 7 d (Figure 4B). Upon resupply of Mn to 9-d-old Mn-starved plants, the abundance of *NRAMP1* transcripts decreased down to the basal level of Mn-replete plants in 3 to 4 d (Figure 4B). We concluded that *NRAMP1* gene expression is regulated by Mn availability and that the response is moderate and slow.

To determine the pattern of expression of *NRAMP1* in the root, we analyzed *NRAMP1* promoter activity by assessing β-glucuronidase (GUS) activity histochemically in transgenic *Arabidopsis* plants expressing the *uidA* gene under the control of the *NRAMP1* promoter. One representative line out of 10 primary transformants analyzed is shown in Figure 4C. In Mn-replete conditions, GUS activity was weakly observed along the root (Figure 4C, panel a), whereas strong GUS staining was observed in the elongation zone of the root when plants were grown under Mn deficiency (Figure 4C, panel b). A cross section in the region with the strongest staining revealed that all the cell layers are stained, including the undifferentiated vascular tissue (Figure 4C, panel c). As the root matures, GUS activity was found to fade away in all cell types, except for a pronounced staining in the vascular cells (Figure 4C, panel d) and in root hairs (Figure 4C, panel e).

NRAMP1 Is a Plasma Membrane Protein

To identify the target membrane of NRAMP1, we followed the localization of the GFP in *nramp1-1* lines producing GFP-tagged NRAMP1, a fusion protein shown above (Figure 3) to rescue the phenotype of the *nramp1-1* mutant. GFP fluorescence, observed by confocal microscopy in roots of 7-d-old plants, labeled the plasma membrane of all the cell layers, consistent with NRAMP1-GFP expression being driven by the 35S promoter. Figure 5 presents the fluorescence observed in a root hair cell, which has the advantage of having well-separated plasma and vacuolar membranes that are therefore easy to distinguish. Indeed, the signal is observed on the membrane surrounding the root hair cell, which is clearly distinct from the tonoplast membrane that delineates small vacuoles visible in the bright-field picture (Figure 5, labeled v). We therefore concluded that the NRAMP1 protein is targeted to the plasma membrane.

Table 1. Elemental Analysis of Shoots and Roots of Wild-Type and *nramp1-1* Plants (μg/g Dry Weight)

			Mn		Fe		Co		Zn		Cu	
Condition	Genotype	Tissue	Mean	SD	Mean	SD	Mean	SD	Mean	SD	Mean	SD
Standard	wild type	shoot	418	22	100	2	0.66	0.04	368	15	6.6	0.2
	nramp1-1		447	25	103	2	0.68	0.08	367	29	6.8	0.2
	wild type	root	290	39	446	86	2.87	0.32	1904	282	13.3	2.1
	nramp1-1		**126**	49	680	170	**1.73**	0.49	1293	236	18.3	6.7
0 Mn	wild type	shoot	13	1	116	7	0.26	0.01	247	15	6.8	0.6
	nramp1-1		**4**	0	130	19	**0.16**	0.01	204	32	9.3	0.6
	wild type	root	6	2	1620	202	0.45	0.07	640	185	11.8	2.3
	nramp1-1		5	2	1836	49	0.42	0.13	1361	686	28.0	11.3

ICP-MS measurement of roots and shoots of wild-type or *nramp1-1* plants grown for 2 weeks in vitro either in standard Mn (20 μM $MnSO_4$) or in Mn-free (no added Mn) medium as indicated ($n = 5$). Significant changes between the wild type and mutant are indicated in bold.

NRAMP1 Mediates in Planta High-Affinity Mn Uptake

Both the tissue and membrane localizations of NRAMP1 were compatible with a function of Mn acquisition from the soil. To test this hypothesis, we assayed Mn uptake in wild-type and *nramp1-1* mutant roots. Plants were grown in hydroponic cultures for 2 weeks in Mn-replete conditions and then transferred to a medium lacking Mn for 1 week to induce Mn acquisition systems. Following Mn resupply, the kinetics of Mn accumulation in roots were measured by atomic absorption spectrometry. We observed a strong decrease in Mn accumulation capacity in *nramp1-1* roots compared with wild-type roots whose Mn content was approximately fivefold greater 10 min after Mn addition (Figure 6A). The level of Mn was restored in the complemented mutant (*nramp1-1*/NRAMP1-GFP line #4) (Figure 6A), indicating that NRAMP1 is required for optimal accumulation of Mn in the roots. Concentration dependence of the Mn uptake obtained in the first 10 min indicated that in *Arabidopsis* wild-type plants, Mn uptake is composed of (1) a saturable uptake system in the low range of Mn concentrations (up to 1 μM) and (2) a linear uptake system in the higher range, likely corresponding to high-affinity and low-affinity transport activities, respectively (Figure 6B). Compared with the wild type, Mn uptake by *nramp1-1* roots was completely lost at low Mn concentrations, whereas at higher concentration of Mn, the uptake by *nramp1-1* paralleled that of the wild type (Figure 6B). This indicates that the *nramp1-1* mutant is defective in high-affinity Mn uptake from the root. The rate of NRAMP1-dependent uptake at low concentrations of Mn was calculated by subtracting the Mn taken up by *nramp1-1* roots from that taken up by wild-type roots (Figure 6C). The data conformed to a Michaelis-Menten function and, when expressed as a double reciprocal Lineweaver-Burk plot, enabled us to calculate an apparent K_m and V_{max} of 28 ± 1 nM and 7.88 ± 0.01 μg/g/10 min, respectively (Figure 6C, inset). We therefore concluded that NRAMP1 catalyzes high-affinity Mn uptake in *Arabidopsis* roots.

NRAMP1 Partially Rescues the Iron Transport-Defective Mutant *irt1-1*

Based on complementation assays in yeast metal transport-defective mutants, NRAMP1 is likely a broad-spectrum metal transporter, including at least Mn and Fe among its substrates. Several studies have shown that *NRAMP1* is also upregulated by Fe deficiency (Curie et al., 2000; Thomine et al., 2000; Colangelo and Guerinot, 2004; see Supplemental Figure 4 online). However, whether NRAMP1 is capable of transporting Fe in vivo cannot be tested easily due to the presence of functional IRT1, whose very strong Fe uptake activity in conditions of Fe limitation is likely to mask a defect of Fe uptake in the *nramp1-1* mutant. We therefore designed a complementation assay in which HA-tagged *NRAMP1*, expressed under the control of the iron deficiency–inducible, root epidermis–specific *IRT1* promoter, was transformed into the loss-of-function mutant *irt1-1*. This HA-NRAMP1 fusion protein was shown to be functional based on the restoration of the growth defect of the *nramp1-1* mutant in low Mn (see Supplemental Figure 1 online). Since absorption of Fe, Zn, Mn, and Co is impaired in *irt1-1* in Fe-limited conditions (Vert et al., 2002), this mutant was used as a plant test tube to investigate the selectivity of NRAMP1 in planta. Immunoblot analysis using anti-HA antibody as a probe confirmed the accumulation of HA-NRAMP1 in roots specifically when grown under Fe deficiency, as shown here for two transgenic lines (Figure 7A). As expected, *irt1-1* plants developed poorly compared with wild-type plants when grown on soil (Figure 7B) or in vitro in iron-limited conditions (Figure 7C). Expression of *NRAMP1* driven by the *IRT1* promoter partially restored *irt1-1* growth (Figures 7B and 7C), suggesting that NRAMP1 can rather efficiently replace IRT1 when produced in IRT1 cell territories.

We next investigated whether the *NRAMP1* transgene could restore *irt1-1* metal content by analyzing elemental content in NRAMP1-complemented *irt1-1* plants. In this experiment, 10-d-old plants were transferred to Fe-free and low Mn medium to (1) induce *IRT1* promoter activity and (2) provide nutritional Mn conditions adapted for optimal transport activity of NRAMP1. Ectopic expression of NRAMP1 in *irt1-1* led to, on average, 60% greater root Fe content compared with untransformed *irt1-1* (Figure 7D). In such Fe-depleted conditions, Fe accumulation was as low in roots of wild-type plants as in *irt1-1*. It is thus remarkable that transgenic NRAMP1-complemented *irt1-1* lines are more efficient at extracting Fe from the soil than wild-type plants.

Consistent with its function in Mn uptake, NRAMP1 restored Mn level in the roots of *irt1-1* (Figure 7C). Similar to Fe, however,

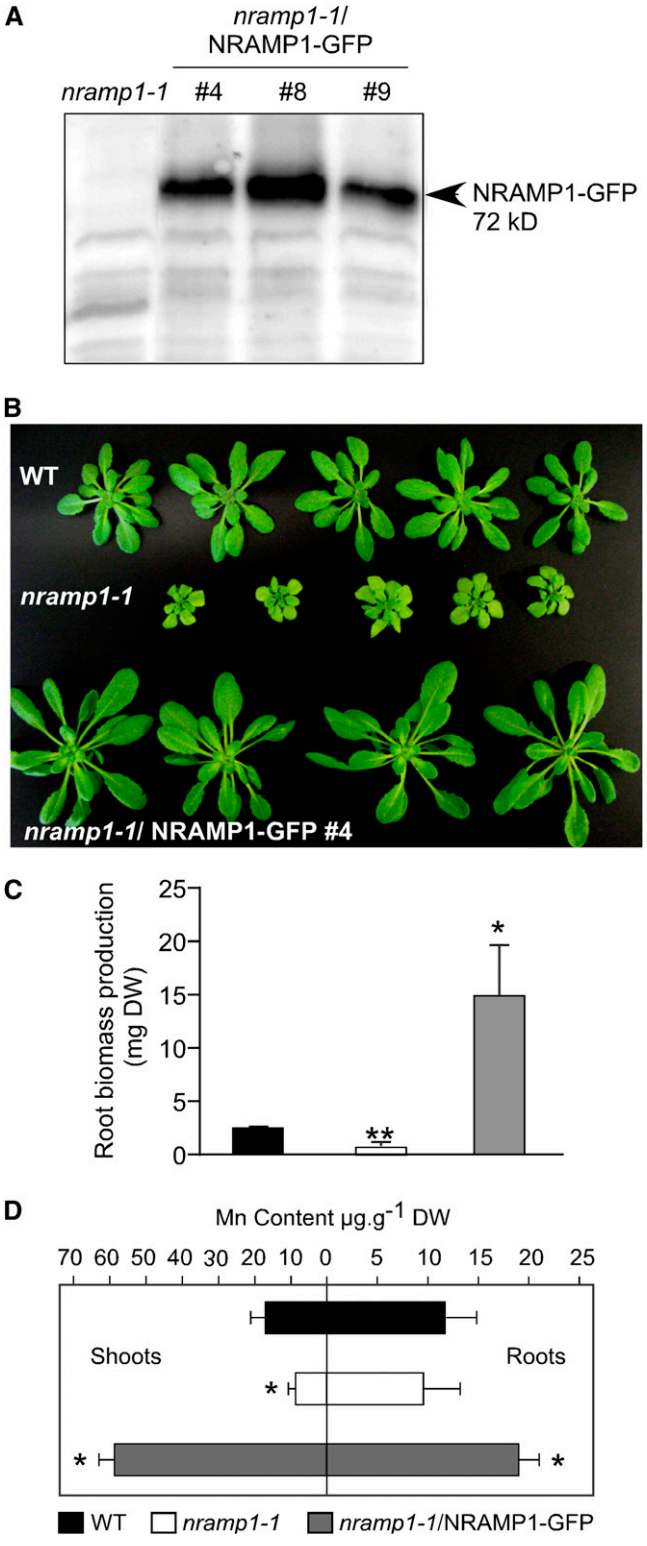

Figure 3. Overproduction of NRAMP1-GFP Rescues *nramp1-1* Hypersensitivity to Mn Deficiency.

(A) Production of NRAMP1-GFP in the *nramp1-1* mutant was controlled by immunoblot analysis of total proteins extracted from roots of either *nramp1-1* or three independent *nramp1-1*–complemented lines probed with a GFP antiserum.

(B) to **(D)** Complementation test. The wild type, *nramp1-1*, and *nramp1-1*–complemented line #4 were grown in Mn-free medium in hydroponic culture for 4 weeks (**B**). In low Mn conditions, NRAMP1-GFP rescues *nramp1-1* growth defect in terms of both shoot **(B)** and root **(C)** biomass production.

(D) ICP-MS measurement of Mn content in roots and shoots of the plants presented in **(B)** and **(C)**, showing that NRAMP1-GFP rescues *nramp1-1* Mn content in low Mn conditions. Both growth and Mn content of the *nramp1-1*/NRAMP1-GFP plants exceed that of wild-type plants (**[C]** and **[D]**) ($n = 4$). Error bars represent SD. Significant differences between the wild type and either *nramp1-1* or *nramp1-1*–complemented line #4 are shown with * $P < 0.01$ in **(C)** and * $P < 0.05$ and ** $P < 0.01$ in **(D)** (Student's *t* test). Data are from one representative experiment ($n = 2$). DW, dry weight.

the Mn-deficient growth condition prevented plants from accumulating large amounts of Mn, thus minimizing the difference of Mn content both between the wild type and *irt1-1* mutant and between *irt1-1* mutant and NRAMP1-complemented *irt1-1* lines. Indeed, when the same experiment was performed in the presence of a 10-fold higher Mn concentration in the culture medium, Mn entry into NRAMP1-complemented *irt1-1* lines increased up to threefold compared with *irt1-1* (see Supplemental Figure 2 online).

Cobalt and zinc are also substrates of IRT1 and are therefore drastically reduced in *irt1-1* roots. Co content was corrected to up to 33% by complementation with NRAMP1 (Figure 7C). Interestingly, although NRAMP1 fails to complement the Zn transport-defective yeast mutant *Δzrt1 Δzrt2* (Lanquar et al., 2004), we measured a slight but statistically significant increase of Zn content in NRAMP1-complemented *irt1-1* lines. This increase, however, restored <10% of the *irt1-1* Zn accumulation defect (Figure 7C). Cu, which is not transported by IRT1, is shown here as a negative control of the experiment. In addition, measurement of metal content in shoots of these plants did not reveal significant differences (see Supplemental Figure 2 online), probably owing to the initial 10-d period of growth in conditions of metal sufficiency that efficiently rescues the *irt1-1* mutant phenotype. Altogether, these data reveal that, in addition to Mn, NRAMP1 is capable of transporting Fe, Co, and, to a lesser extent, Zn into the root.

DISCUSSION

It is commonly accepted that the physiological requirement for Mn in living cells is low and that the uptake capacity exceeds that requirement by several orders of magnitude (Rengel, 2000), thus indicating a poor regulation of Mn uptake. In this work, we identified two separate Mn uptake systems in the root of the model plant *Arabidopsis*, mediating high-affinity Mn influx at concentrations of up to 1 μM and low-affinity Mn influx at higher concentrations. In addition, we demonstrate the absolute requirement for this root high-affinity Mn transport system to acquire Mn when poorly available and show that this activity is catalyzed by the metal transporter NRAMP1. Indeed, we found

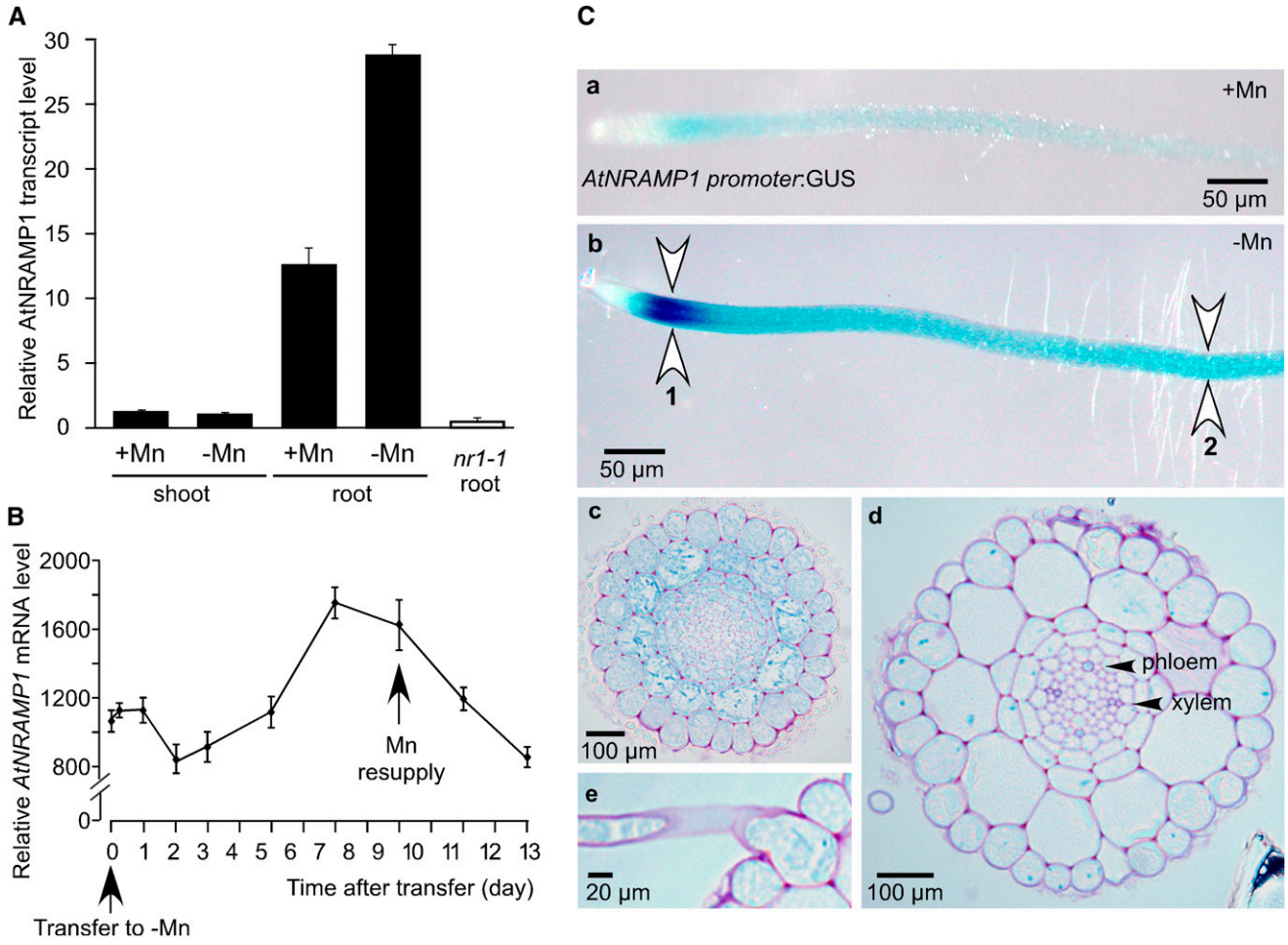

Figure 4. Expression Analysis of *NRAMP1*.

(A) Relative *NRAMP1* transcript abundance, determined by real-time RT-PCR, in roots and shoots of wild-type plants grown in vitro for 2 weeks either in Mn-replete medium or in Mn-free medium; *NRAMP1* mRNA level in the *nramp1-1* (*nr1-1*) mutant is shown as a negative control.

(B) Kinetics of the response of *NRAMP1* to Mn deficiency and Mn resupply monitored by real-time RT-PCR in roots of plants grown in vitro. Data are means of one representative experiment (**[A]**, $n = 3$; **[B]**, $n = 4$). Error bars represent SD.

(C) Histochemical staining of GUS activity in the root of an *Arabidopsis* line transformed with the construct Pro*NRAMP1*:GUS. **(a)** and **(b)** GUS staining of the primary root of 2-week-old plants grown in vitro either in Mn-replete conditions **(a)** or in Mn-free medium **(b)**; 1, elongation zone; 2, absorption zone. **(c)** to **(e)** Cross sections of a root grown and stained as in **(b)** in the elongation zone **(c)**, in the mature zone **(d)**, or at the level of a root hair **(e)**.

that the *Arabidopsis nramp1-1* loss-of-function mutant exhibits a complete loss of root Mn uptake capacity exclusively in the low concentration range of Mn supply, resulting in poor growth of the plant under low Mn supply. This phenotype is associated with a drastic reduction of the amount of Mn in *nramp1-1* tissues. All of these defects are fully rescued by complementation of the *nramp1-1* mutant with *NRAMP1* cDNA. Consistent with a role of NRAMP1 in the acquisition of Mn by the root are the findings that (1) NRAMP1 is a plasma membrane protein, based on fluorescence analysis of NRAMP1-GFP–producing plants, (2) *NRAMP1* gene expression is specific to the root and regulated by Mn availability, and (3) plants overexpressing *NRAMP1* exhibit enhanced growth and increased Mn content in Mn-limiting conditions.

NRAMP1 presents the characteristics of a high-affinity Mn transporter, with an apparent K_m of 28 nM. This very low K_m value is compatible with the appearance of deficiency symptoms in the *nramp1-1* mutant only in conditions of drastic Mn starvation. Two Mn uptake systems have also been described in barley roots where the K_m value for the high-affinity uptake was estimated to be around 2 to 5 nM (Pedas et al., 2005). Interestingly, an increased rate of Mn uptake was measured in a Mn-efficient genotype of barley, compared with a Mn-inefficient genotype, and has been shown to correlate with increased Hv *IRT1* expression (Pedas et al., 2005, 2008). Since Hv *IRT1* was the only clone isolated from screening a root cDNA library for its ability to restore Mn uptake of the yeast *smf1* mutant, it was speculated that IRT1 might contribute to high-affinity Mn uptake in this

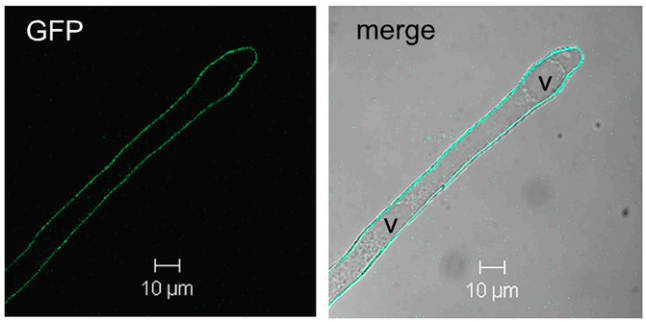

Figure 5. NRAMP1 Is a Plasma Membrane Protein.

Confocal microscopy observation of the membrane localization of the NRAMP1-GFP fusion protein in a root hair of the NRAMP1-GFP–complemented *nramp1-1* line #4 presented in Figure 3. Plants were grown for 7 d in vitro in standard medium prior to the observation. v, vacuole.

species. Nevertheless, based on our results that establish the essential role of NRAMP1 in high-affinity Mn acquisition in *Arabidopsis*, a similar role for barley NRAMP homologs should be considered.

The biological function of the NRAMP transporters in Fe homeostasis has been widely shown in mammals, in particular for the NRAMP2/DCT1/DMT1 members that mediate pH-dependent uptake of Fe^{2+}. Knocking out *NRAMP2* results in microcytic anemia in rat or mouse (Fleming et al., 1997, 1998). That NRAMP homologs are also physiological transporters of Mn has been demonstrated in prokaryotes with the MntH transporter and in *S. cerevisiae* with Smf1p and Smf2p (Supek et al., 1996; Kehres et al., 2000; Makui et al., 2000). In higher eukaryotes, by contrast, Mn transport activity of NRAMP has been inferred only based on functional complementation of Mn uptake yeast mutants and alterations of Mn metabolism in knockout animals because a clear demonstration of such Mn transport activity in vivo has proven difficult (Au et al., 2008). For instance, the requirement of DMT1 for olfactory Mn uptake, the main route of Mn entry into the brain (Thompson et al., 2007), has been contradicted in a study showing no alteration of Mn brain uptake in the *DMT1*-disrupted Belgrade rats (Crossgrove and Yokel, 2004). Because *Arabidopsis* NRAMP1 is located at the plasma membrane of most root cells and performs acquisition into the root, we were able to measure changes in the net influx of Mn in the *nramp1-1* mutant and thus demonstrate that a NRAMP homolog from a higher eukaryote functions as a physiological Mn transporter.

NRAMP1 is capable of transporting both Mn and Fe when heterologously expressed in yeast (Curie et al., 2000; Thomine et al., 2000; Lanquar et al., 2004; Cailliatte et al., 2009). At first sight, however, NRAMP1 appeared more selective in planta, since we found that the inactivation of *NRAMP1* alters Mn homeostasis but not Fe homeostasis. Early on, we reported that *NRAMP1* overexpressor lines are hypertolerant to toxic Fe concentrations (Curie et al., 2000). This phenotype is likely indirect because Mn content, which is increased in these lines (Figure 3C), might either compete with tissue Fe content, therefore minimizing Fe toxicity for the plant, or protect against Fenton chemistry. To reconcile the data obtained in yeast and in planta, a possible explanation could be that although both Fe and Mn are acceptable substrates for NRAMP1, its selectivity in planta might be governed by the availability of each metal in the root apoplast. Alternately, the Fe transport activity of NRAMP1 could be masked by a redundant transporter, such as IRT1. This hypothesis is supported by our data showing that overexpression of *NRAMP1* partially rescued the phenotype of the *irt1-1* loss-of-function mutant, restoring partly its growth and Fe content in conditions of Fe deficiency.

The *irt1-1*/NRAMP1 plants have made it possible to test the transport of Co and Zn in addition to Fe. We found that ectopic expression of *NRAMP1* rescued <10% of the Zn uptake defect of *irt1-1* in Fe-deficient conditions. Together with the absence of functional complementation of the yeast Zn uptake mutant *Δzrt1Δzrt2* by NRAMP1 (Lanquar et al., 2004), this result suggests that NRAMP1 does not transport Zn efficiently. On the contrary, Co content was more significantly restored in the two *irt1-1*/NRAMP1 lines, indicating that, along with Mn and Fe, Co is an acceptable substrate for NRAMP1 in vivo. This finding is consistent with the decrease of Co concentration measured in the *nramp1-1* mutant (Table 1). The *frd3* mutant exhibits alteration of Fe homeostasis owing to a defect of citrate efflux in the vascular tissue, the consequence of which is a decrease of Fe mobility in the plant (Rogers and Guerinot, 2002; Durrett et al., 2007). In addition, the hallmark of the *frd3* mutant is a strong overaccumulation of Mn and Co (Delhaize, 1996; Lahner et al., 2003). Despite being upregulated in *frd3*, IRT1 alone might not account for the increase of Mn and Co because Zn, which is also a substrate of IRT1, is not modified in *frd3*. Instead, Mn and Co correspond typically to the in planta substrates of NRAMP1. Therefore, the possible deregulation of *NRAMP1* in the *frd3* mutant should be tested in the future to investigate the contribution of NRAMP1 to the *frd3* phenotype.

Transporters of the NRAMP family are often capable of transporting nonessential and toxic metals, such as cadmium (Cd) and lead (Pb). Mammalian DCT1 was shown to mediate active transport of Cd^{2+} in *Xenopus laevis* oocytes (Gunshin et al., 1997); however, this function still awaits in vivo confirmation since *mk*/*mk* mice that are mutated in DCT1 accumulate as much intestinal Cd as wild-type mice (Suzuki et al., 2008). In *Arabidopsis*, NRAMP1, 3, 4, and 6 were shown to confer Cd sensitivity in yeast (Thomine et al., 2000; Cailliatte et al., 2009). We recently reported that knocking out *NRAMP6* produces plants with increased tolerance to Cd and that, consistently, overexpression of *NRAMP6* generates plants with increased sensitivity to Cd (Cailliatte et al., 2009). In this study, we have shown that *nramp1-1* plants grown in low Mn conditions are less sensitive to a cadmium treatment than wild-type plants, suggesting that NRAMP1 is capable of mediating Cd entry in *Arabidopsis* (see Supplemental Figure 3 online). Modification of *NRAMP3* and *NRAMP4* expression in *Arabidopsis* also results in changes in Cd tolerance, albeit in the opposite direction compared with NRAMP1 and NRAMP6; the double *nramp3 nramp4* mutant exhibits hypersensitivity to Cd (Oomen et al., 2009), presumably as a result of a general defect of metal remobilization from the vacuole, which may be required for Cd tolerance.

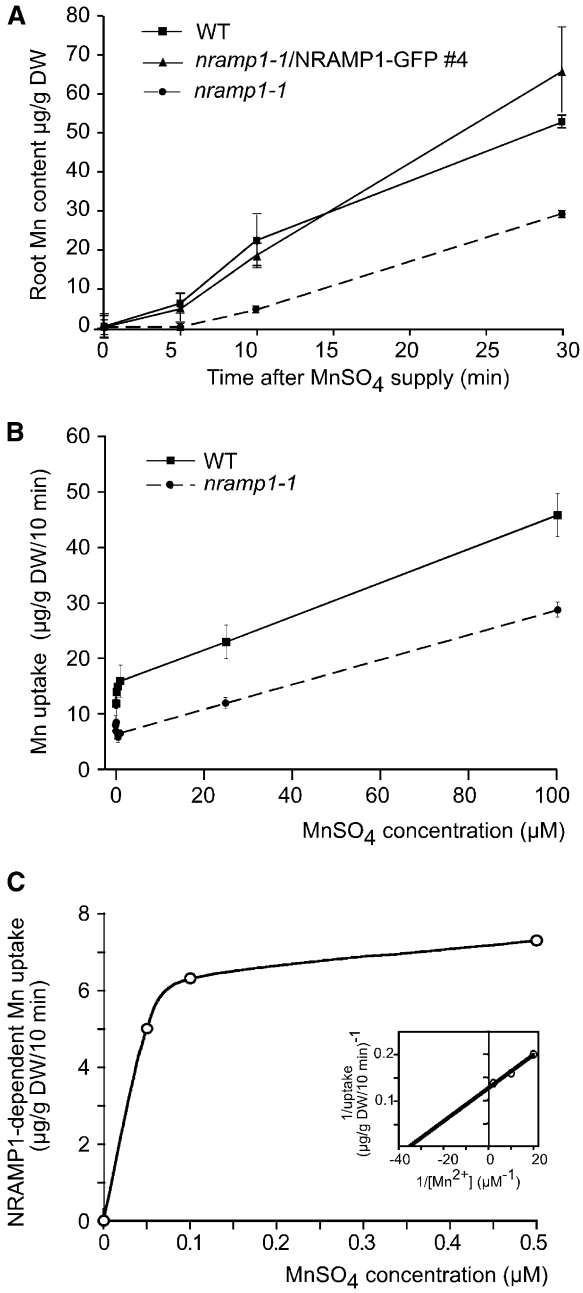

Figure 6. Root High-Affinity Mn Uptake Is Defective in the *nramp1-1* Mutant.

(A) Time dependence of Mn accumulation in the wild type, *nramp1-1*, and *nramp1-1*–complemented line #4. Plants were grown in Mn-replete hydroponic culture for 2 weeks and then transferred to Mn-free medium for 1 week prior to the assay. At the time point 0, plants were supplemented with 18 μM $MnSO_4$. Roots were harvested at the time points indicated in the figure and washed with $CaNO_3$/bathophenanthroline disulphonate prior to Mn measurement by atomic absorption spectrometry.

(B) Concentration-dependent Mn uptake at 10 min by wild-type and *nramp1-1* roots.

(C) NRAMP1-dependent uptake. The rate of NRAMP1-dependent uptake was calculated by subtracting the amount of Mn taken up by *nramp1-1* roots from that taken up by wild-type roots. The data were fitted to a Michaelis-Menten function by nonlinear least squares analysis. The apparent K_m and V_{max} were calculated by expressing the data in the form of a double reciprocal Lineweaver-Burk plot (inset). Values shown are means ± SD (n = 3) of one representative experiment (n = 2). DW, dry weight.

In contrast with other trace elements, the absorption of Mn is not well regulated, and there is little evidence of homeostatic mechanisms that regulate uptake and efflux of Mn. Here, we report that *NRAMP1* harbors a pattern of expression typical of an acquisition transporter, including induction in response to substrate deficiency and repression upon resupply. Following transfer of the plants to –Mn, a transient inhibition of *NRAMP1* transcript accumulation was observed. This is reminiscent of the pattern of response of *IRT1* to Fe, which has been attributed to Fe being locally required for the response (Vert et al., 2003). This suggests that Mn could act as a local inducer of the *NRAMP1* response to Mn deficiency. In *C. reinhardtii*, one of the two NRAMP homologs, NRAMP1, is induced in Mn-deficient cells and repressed by Mn supplementation, which suggests a role of NRAMP1 in Mn acquisition in green algae (Allen et al., 2007). The finding that the intensity of the response of *NRAMP1* to Mn deficiency is quite low may imply that additional levels of regulation ensure proper expression of *NRAMP1*. *SMF1*, its yeast putative ortholog, is regulated by environmental Mn but only at the posttranslational level. Smf1p is stabilized at the plasma membrane under Mn deficiency, whereas a bulk of the protein is degraded in the vacuole in response to physiological or excess amount of Mn (Liu and Culotta, 1999; Jensen et al., 2009). We tested the effect of supplying NRAMP1-GFP–expressing plants with an excess of Mn (1 mM $MnSO_4$); however, no switch of NRAMP1 membrane localization was observed. We found the kinetics of the *NRAMP1* response to –Mn to be slow, reaching a maximum of induction after 7 d of Mn starvation. This matches the late appearance of symptoms in the Mn-starved *nramp1-1* mutant. Moreover, it correlates well with the usually high tolerance of plants to Mn deficiency, which probably reflects the difficulty to deplete Mn stores in plant tissues.

NRAMP1 expression, based on its promoter activity, is specific to the root, consistent with a function of acquisition from the soil, and lies in most cell layers. This suggests that inner layers of root cells may contribute to Mn uptake, a feature that is unusual since assimilation of nutrients is generally performed by the epidermis and cortex. Interestingly, in the *Arabidopsis* mutant *Enhanced suberin1*, which contains increased root suberin, several ions including Mn were shown to be greatly decreased in the shoot, suggesting that the radial movement of Mn occurs for a significant part through the apoplast (Baxter et al., 2009). We also detected a strong *NRAMP1* promoter activity in root hairs. Given that Mn deficiency triggers a substantial increase in the number of root hairs in *Arabidopsis* (Yang et al., 2008), we can speculate that the lack of a strong regulation of *NRAMP1* in response to Mn deficiency is counterbalanced by an increase of *NRAMP1*-expressing root hairs.

The expression of *NRAMP1* is also regulated by Fe availability. The transcripts of *NRAMP1* or Le *IRT1* accumulate at higher level

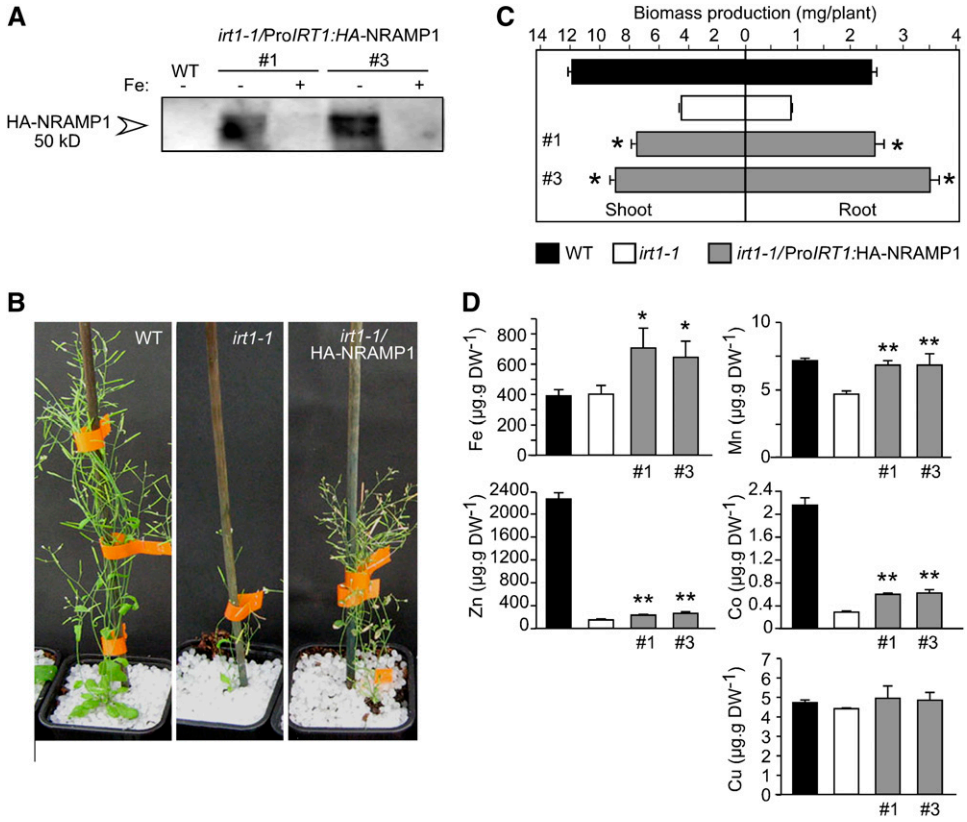

Figure 7. NRAMP1 Partially Rescues *irt1-1* Harboring a Broad Metal Selectivity in Vivo.

(A) *irt1-1*/Pro*IRT1*:HA-NRAMP1 transgenic lines #1 and 3 produce the HA-NRAMP1 fusion protein in Fe-deficient roots. Plants were grown in vitro in Fe-replete (50 μM FeEDTA) or Fe-limited (10 μM Fe-EDTA) medium for 2 weeks. Total protein extracts were immunoblotted and hybridized to an anti-HA antibody.
(B) and **(C)** NRAMP1 partially restores growth of *irt1-1* under Fe deficiency.
(B) Phenotype of the wild type, *irt1-1*, and *irt1-1*/Pro*IRT1:HA*-NRAMP1 line #1 grown in soil for 5 weeks.
(C) Root and shoot biomass of the wild type, *irt1-1*, or *irt1-1*/Pro*IRT1:*HA-NRAMP1 lines #1 and 3 grown in vitro in Fe-limited conditions as in **(A)**.
(D) NRAMP1 partially rescues Fe, Co, and Zn uptake defects of the *irt1-1* mutant. Elemental analysis performed by ICP-MS on roots of the wild type, *irt1-1*, or *irt1-1*Pro*IRT1:*HA-NRAMP1 lines #1 and 3 grown in vitro for 10 d in metal replete medium and then transferred to Fe-free (no added Fe) or Mn-limiting (0.5 μM $MnSO_4$) conditions for five additional days. Error bars represent SD. Significant differences between *irt1-1* and the complemented lines are indicated by * $P < 0.05$ and ** $P < 0.01$. $n = 4$ **(C)** or $n = 10$ **(D)**. One representative experiment ($n = 2$) is shown in **(C)** and **(D)**. DW, dry weight.

in iron starvation regimes (Curie et al., 2000; Thomine et al., 2000; Bereczky et al., 2003; Colangelo and Guerinot, 2004). Consistently, we found GUS activity driven by the *NRAMP1* promoter to be, on average, 4.5 times greater in Fe-deficient compared with Fe-replete conditions (see Supplemental Figure 4 online). Moreover, the Fe regulation is lost for *NRAMP1* and Le *NRAMP1* in the *Arabidopsis fit* and tomato (*Solanum lycopersicum*) *fer* loss-of-function mutants, respectively (Bereczky et al., 2003; Colangelo and Guerinot, 2004), suggesting that NRAMP1 is modulated by the master regulator FIT/FER of the iron deficiency response. These observations support the idea that NRAMP1 plays a role in the root response to conditions of low availability of iron, either by contributing to Fe uptake or by promoting the acquisition of Mn, which is known to be associated with iron starvation growth conditions (Vert et al., 2002). Alternately, –Fe-dependent upregulation of *NRAMP1* might be a secondary effect of the –Fe-mediated changes in internal Mn availability. However, this is unlikely since external Fe deficiency triggers an increase in Mn concentration in plant tissues, whereas it is a decrease of Mn that will result in the activation of *NRAMP1* expression.

We show here that *Arabidopsis* growth under Mn deficiency depends on the presence of a high-affinity Mn uptake system that is catalyzed by NRAMP1 and that *NRAMP1* gene expression is modulated by Mn availability. IRT1 also transports Mn efficiently and is overproduced in calcareous soils, which represent conditions of poor availability of Fe, but also Mn. Therefore, the question arises as to the redundancy of these two Mn uptake systems in the root of *Arabidopsis*. It is possible that IRT1 and NRAMP1 have different affinity constants for Mn, thus justifying the need for two parallel systems of Mn uptake. Alternately, IRT1 and NRAMP1 might act in different tissues of the root, as suggested by their pattern of expression, indicating that *IRT1* is exclusively expressed in external layers of the absorption zone of the root, whereas *NRAMP1* expression is more widespread

along the root and includes cells of the inner layers. If Mn uses an apoplastic route to move radially in the root (Baxter et al., 2009), it is conceivable that IRT1 and NRAMP1 cooperate, transporting Mn sequentially from the outer cells to the central cylinder of the root to eventually feed the aerial parts. In future work, generating an *nramp1 irt1* double mutant may help clarify the respective contribution of NRAMP1 and IRT1 to Mn acquisition.

In conclusion, our study demonstrates that a member of the NRAMP family of metal transporters from higher eukaryotes is a physiological transporter of Mn that is essential for growth in conditions of low Mn availability. These results therefore bring credit to the still controversial contribution of Nramp2/DCT1/DMT1 to Mn transport in mammals (Au et al., 2008). More generally, our study highlights the importance of a high-affinity Mn transport system in sustaining the growth of a multicellular organism, a function that has often been underestimated on the grounds that Mn deficiency is rare due to low Mn requirements. The general belief that Mn uptake rates are not limiting therefore may not be accurate in many species.

METHODS

Plant Material and Growth Condition

Arabidopsis thaliana plants (ecotype Columbia-0, except for the *irt1-1* mutant isolated in the Wassilewskija ecotype background) were grown in vitro in sterile conditions at 21°C with 16-h-light/8-h-dark cycles. Seeds were surface sterilized and sown on half-strength Murashige and Skoog medium containing 1% sucrose and either 0.6% agar for horizontal cultures or 1% agar for vertical cultures. The medium was buffered with 0.5 $g \cdot L^{-1}$ MES, and its pH was adjusted to 5.7 with KOH. When indicated, metals were subtracted from the microelements solution to enable deficiency tests. All reagents were purchased from Sigma-Aldrich. For hydroponic cultures, *Arabidopsis* plants were grown hydroponically in a controlled environment (8 h light 23°C/16 h dark 20°C cycles, 300 $\mu E \cdot s^{-1}$ light intensity, 70% relative humidity) for the amount of time indicated in the legend of the figures in a nutrient solution containing 0.25 mM Ca $(NO_3)_2$, 1 mM KH_2PO_4, 0.5 mM KNO_3, 1 mM $MgSO_4$, 50 μM Fe(III)-Na-EDTA, 50 μM H_3BO_3, 18 μM $MnSO_4$, 1 μM $CuSO_4$, 10 μM $ZnSO_4$, and 0.02 μM MoO_4Na_2. The pH was adjusted to 5.5 with MES. The nutrient solution was renewed weekly for the first 2 weeks and every 2 d from the third week on. For the uptake assay, the solution was also renewed the day before the assay. The pH stability of the culture medium was verified regularly. For growth in soil in the greenhouse, plants were cultivated on Humin substrate N2 (Neuhaus) at 23°C with a sunlight intensity limited to 300 $\mu mol \cdot m^{-2} \cdot s^{-1}$ and 16-h-light/8-h-dark cycles.

The *nramp1-1* mutant was isolated as a T-DNA insertion mutant line SALK_053236 from the SIGnAL T-DNA collection (http://signal.salk.edu/).

Arabidopsis plants were transformed using the GV3101 strain of *Agrobacterium tumefaciens* according to the floral dip protocol (Clough and Bent, 1998). Transformed seeds were selected based on resistance to either kanamycin (50 $mg \cdot L^{-1}$) for the ProNRAMP1:GUS construct, Basta (10 $mg \cdot L^{-1}$) for the 35S:NRAMP1-GFP construct, hygromycin (50 $mg \cdot L^{-1}$) for the Pro*IRT1*:HA-NRAMP1 construct, or based on the fluorescence of the seeds (http://www.isv.cnrs-gif.fr/jg/alligator/intro.html) for the 35S:HA-NRAMP1 construct in the pFP101 vector.

Root Length Measurements

Plants grown vertically on square Petri dishes were scanned at the indicated times, and root length was determined using the OPTIMAS V6.0 program. Continuous variables were expressed as means ± SD. Statistical differences between the genotypes were evaluated by performing a Student's *t* test ($P < 0.001$).

Plasmid Constructs

For *nramp1-1* complementation tests, *NRAMP1* cDNA was amplified by PCR using primers OCC1 (5′-ATAAGAATGCGGCCG CATGACTAG-TATGGCGGCTACAGGATCTGGAC-3′), encompassing the ATG initiation codon, and OCC2 (5′-ATAGTTTAGCGGCCGCTCAGTCGACGCTAGC-GTCAACATCGGAGGTAGAT-3′), encompassing the TGA stop codon. Both primers introduce a *Not*I site at the fragment extremities. In addition, OCC1 introduces an in-frame *Nhe*I site immediately downstream the *NRAMP1* ATG initiation codon. The amplified fragment was cloned into the *Not*I site of the pFL61 yeast expression vector. A two-copy fragment of the hemagglutinin epitope (HA) carrying *Xba*I extremities was subsequently inserted in the *Nhe*I site of the resulting construct to produce NRAMP1 protein tagged with HA at its N terminus (construct pFL61/HA-NRAMP1). The HA-NRAMP1 cassette was then subcloned as a blunt fragment into the blunted *Sal*I site of the pFP101 plant stable expression vector downstream of the CaMV *35S* promoter (http://www.isv.cnrs-gif.fr/jg/alligator/).

For the 35S:NRAMP1-GFP fusion construct, the NRAMP1 cDNA was amplified without its stop codon and cloned into the pDNOR 207 entry vector (Gateway; Invitrogen) as part of the ORFEOME project (http://urgv.evry.inra.fr/orfeome/). NRAMP1 cDNA was subsequently fused with GFP by recombination with the destination vector pG0229-GFP (Lurin et al., 2004) to generate a C-terminal GFP fusion of NRAMP1 protein.

For the Pro*NRAMP1*:GUS construct, 1.65 kb of genomic sequence located upstream of the *NRAMP1* initiation codon was amplified by PCR from *Arabidopsis* BAC F23A5 using primers OCC42 (5′-AATCATGTCT-TAAGCTTCATTAC-3′) and OCC44 (5′-GCCGCCATGGCCGTCTCT-CTC-3′), introducing a *Hind*III site and a *Nco*I site, respectively. The amplified promoter fragment was translationally fused to the *uidA* gene, encoding GUS, by cloning into the *Hind*III and *Nco*I sites of the pGUS vector (Eyal et al., 1995). The Pro*NRAMP1*-GUS cassette was then subcloned as a *Hind*III-*Xba*I fragment into the pBIN19 plant binary vector (Bevan, 1984) opened with the same restriction sites.

For construction of the Pro*IRT1*:HA-NRAMP1 plasmid for complementation of the *irt1-1* mutant, 990 bp of the *IRT1* sequence upstream of the ATG were cloned in the pCHF3 vector as an *Eco*RI-*Bam*HI fragment in place of the CaMV*35S* promoter. The *Eco*RI-*Hind*III fragment of the resulting plasmid, containing the *IRT1* promoter and the *RbcS* terminator, was subcloned into the same restriction sites of the pGreen179 binary vector, which confers hygromycin resistance in transgenic plants. The polylinker sites in 5′ of the *IRT1* promoter, situated between the *Not*I and *Eco*RI sites, were then eliminated to generate pGreen179/Pro*IRT1*. The HA-NRAMP1 *Not*I fragment digested from the pFL61/HA-NRAMP1 construct described above was inserted as a blunt fragment into the Klenow-blunted *Bam*HI site of pGreen179/Pro*IRT1* in between the *IRT1* promoter and the *RbcS* terminator to produce the Pro*IRT1*:HA-NRAMP1 construct.

GUS Histochemical Analysis

Pro*NRAMP1*:GUS transgenic lines were grown in hydroponics under Mn-deficient (no added Mn) conditions. Plants were harvested after 2 to 4 weeks, soaked in phosphate buffer (50 mM $NaPO_4$ and 0.05% Triton X-100, pH 7.2), and then prefixed by vacuum infiltrating the plants for 45 min in phosphate buffer containing 4% formaldehyde. After three washes in phosphate buffer, samples were incubated 16 h at 37°C in GUS buffer containing 50 mM $NaPO_4$, 0.5 mM ferrocyanide, 0.5 mM ferricyanide, 0.05% Triton X-100, pH 7.2, and 1 mM 5-bromo-4-chloro-3-indolyl-β-D-glucuronide. Samples were then either cleared with successive baths of increasing ethanol concentrations from 50 to 100% for direct observation

or embedded in hydroxyethylmethacrylate (Technovit 7100; Heraus-Kulzer). Thin cross sections (3 μm) were cut using a Leica RM 2165 microtome, counterstained with the Schiff dye, and observed with an Olympus BH2 microscope.

Gene Expression

Total RNA was extracted using the TRIZOL reagent (Invitrogen) following the manufacturer's instructions. Samples were treated with DNase (Promega) to eliminate genomic DNA contamination. Three micrograms of DNA-free RNA was used for reverse transcription by the MMLV-RT (Promega) with anchored oligo(dT_{23}). Real-time PCR was performed using the LightCycler FastStart DNA Master^{PLUS} SYBR GREEN I (Roche), using the following gene-specific primers: *Actin*-F, 5′-GGTAACATT-GTGCTCAGTGGTGG-3′; *Actin*-R, 5′-AACGACCTTAATCTTCATGC-TGC-3′; At *NR1*-F, 5′-GTAGCCACTTCTCTTCTTATTTCAAG-3′; and At *NR1*-R, 5′-ACCTTTATTCTAGTACACTATCGAAAG-3′. Primer specificity was confirmed by analysis of the melting curves and agarose gel electrophoresis of the PCR products. Relative transcript levels were calculated relative to the transcript amount of the constitutively expressed *ACT2* gene (At3g18780) as follows: RTL = $1000*2^{-\Delta Ct}$.

Isolation of Proteins and Protein Gel Blot Analysis

Total proteins were extracted by grinding 100 mg of tissue in 300 μL of extraction buffer (50 mM Tris-HCl, pH 8, 5% SDS, 5% β-mercaptoethanol, 25 mM EDTA, and 0.1% phenylmethylsulfonyl fluoride) in liquid nitrogen, followed by centrifugation at 4°C for 15 min at 14,000*g*. Thirty micrograms of total proteins were separated on SDS-PAGE gel and electroblotted to a Hybond-P membrane (Amersham Biosciences). Membranes were blocked overnight in 1× PBS, 0.1% Tween 20 containing 0.2% blocking reagent (Aurora protein gel blot chemilumiescence detection system; ICN Biochemicals). Immunodetection of NRAMP1-GFP was performed using rabbit polyclonal anti-GFP antibodies (A6455; Invitrogen) at 1:3000 dilution for 1 h at room temperature. Immunodetection of HA-NRAMP1 was performed using a mouse anti-HA monoclonal antibody (12CA5; Roche Applied Science) at a 1:4000 dilution. IgG conjugated to alkaline phosphatase (Promega) was used as a secondary antibody. Alkaline phosphatase activity was revealed by incubating the membranes in chemiluminescent AP substrate (Millipore) according to the manufacturer's instructions. Membranes were exposed to BioMax XAR films (Kodak).

Mn Uptake Assay

Mn uptake assays were performed on plants grown hydroponically in Mn-replete conditions for 2 weeks and then transferred to Mn-free medium for 1 week for optimal NRAMP1 expression/activity. At t_0, Mn-starved plants were transferred to medium containing 18 μM $MnSO_4$, and roots were harvested at the time points indicated in the figure. Root samples were washed for 10 min at 4°C in 2 mM $CaSO_4$ and 10 mM EDTA to remove apoplastic Mn and avoid active efflux of the metal as described by Lasat et al. (1996). Samples were rinsed three times in water, paper blotted, and placed into preweighed Pyrex tubes for mineralization.

Elemental Analyses

Roots were desorbed by washing for 10 min with 2 mM $CaSO_4$ and 10 mM EDTA and for 3 min with 0.3 mM bathophenanthroline disulphonate and 5.7 mM sodium dithionite and were then rinsed twice in deionized water. Shoots were simply rinsed twice with deionized water. Samples were dried at 80°C for 2 d. For mineralization, tissues were digested completely (1 to 3 h) in 70% HNO_3 at 120°C. For Mn uptake assays, Mn measurement was performed by atomic absorption spectrometry (SpectrAA220-FS; Varian). For phenotypic analysis of the mutants, elemental analyses were performed by ICP-MS.

Fluorescence Imaging

nramp1-1 lines transformed with the NRAMP1-GFP construct were grown vertically in half-strength Murashige and Skoog medium for 7 d. GFP fluorescence was observed using a confocal microscope (LSM510 Meta; Zeiss). The excitation wavelength was 488 nm, and emission wavelength was between 500 and 530 nm.

Accession Numbers

Sequence data from this article can be found in the Arabidopsis Genome Initiative or GenBank/EMBL databases under accession numbers At1g80830 (*NRAMP1*), At4g19690 (*IRT1*), and At3g18780 (*ACT2*).

Supplemental Data

The following materials are available in the online version of this article.

Supplemental Figure 1. Overproduction of NRAMP1-HA Rescues *nramp1-1* Hypersensitivity to Mn Deficiency.

Supplemental Figure 2. NRAMP1 Partially Rescues Metal Content in the *irt1-1* Mutant.

Supplemental Figure 3. Overproduction of HA-NRAMP1 Rescues *nramp1-1* Hypersensitivity to Mn Deficiency.

Supplemental Figure 4. *NRAMP1* Promoter Activity Increases in Response to Fe Deficiency.

ACKNOWLEDGMENTS

We thank Veronique Vacchina and Ryszard Lobinsky (Laboratoire de Chimie Analytique Bio-Inorganique et Environnement, University of Pau, France) for their assistance with ICP-MS analyses and Jean-Baptiste Thibaut (Laboratoire de Biochimie et Physiologie Moléculaire Végétale, Montpellier, France) for his advice in the determination of uptake kinetics parameters. We also thank Claire Lurin and Ian Small (Unité de Recherche en Génomique Végétale, Evry, France) for their gift of the pDONR207/NRAMP1 construct and Daniel Couch for critical reading of the manuscript. This work was funded by GENOPLANTE (Project AF 2001065) and the Centre National de la Recherche Scientifique. R.C. was supported by the French Ministry of Agriculture and Fisheries, and A.S. was supported by the French Ministry of Education and Research and by the Institut National de la Recherche Agronomique.

Received November 25, 2009; revised February 10, 2010; accepted February 26, 2010; published March 12, 2010.

REFERENCES

Allen, M.D., Kropat, J., Tottey, S., Del Campo, J.A., and Merchant, S.S. (2007). Manganese deficiency in Chlamydomonas results in loss of photosystem II and MnSOD function, sensitivity to peroxides, and secondary phosphorus and iron deficiency. Plant Physiol. **143:** 263–277.

Au, C., Benedetto, A., and Aschner, M. (2008). Manganese transport in eukaryotes: the role of DMT1. Neurotoxicology **29:** 569–576.

Baxter, I., Hosmani, P.S., Rus, A., Lahner, B., Borevitz, J.O., Muthukumar, B., Mickelbart, M.V., Schreiber, L., Franke, R.B., and Salt, D.E. (2009). Root suberin forms an extracellular barrier that

affects water relations and mineral nutrition in Arabidopsis. PLoS Genet. **5:** e1000492.

Belouchi, A., Cellier, M., Kwan, T., Saini, H.S., Leroux, G., and Gros, P. (1995). The macrophage-specific membrane protein Nramp controlling natural resistance to infections in mice has homologues expressed in the root system of plants. Plant Mol. Biol. **29:** 1181–1196.

Belouchi, A., Kwan, T., and Gros, P. (1997). Cloning and characterization of the OsNramp family from *Oryza sativa*, a new family of membrane proteins possibly implicated in the transport of metal ions. Plant Mol. Biol. **33:** 1085–1092.

Bereczky, Z., Wang, H.Y., Schubert, V., Ganal, M., and Bauer, P. (2003). Differential regulation of nramp and irt metal transporter genes in wild type and iron uptake mutants of tomato. J. Biol. Chem. **278:** 24697–24704.

Bevan, M. (1984). Binary Agrobacterium vectors for plant transformation. Nucleic Acids Res. **12:** 8711–8721.

Cailliatte, R., Lapeyre, B., Briat, J.F., Mari, S., and Curie, C. (2009). The NRAMP6 metal transporter contributes to cadmium toxicity. Biochem. J. **422:** 217–228.

Clough, S.J., and Bent, A.F. (1998). Floral dip: A simplified method for Agrobacterium-mediated transformation of *Arabidopsis thaliana*. Plant J. **16:** 735–743.

Colangelo, E.P., and Guerinot, M.L. (2004). The essential basic helix-loop-helix protein FIT1 is required for the iron deficiency response. Plant Cell **16:** 3400–3412.

Crossgrove, J.S., and Yokel, R.A. (2004). Manganese distribution across the blood-brain barrier III. The divalent metal transporter-1 is not the major mechanism mediating brain manganese uptake. Neurotoxicology **25:** 451–460.

Crowley, J.D., Traynor, D.A., and Weatherburn, D.C. (2000). Enzymes and proteins containing manganese: An overview. Met. Ions Biol. Syst. **37:** 209–278.

Curie, C., Alonso, J.M., Le Jean, M., Ecker, J.R., and Briat, J.F. (2000). Involvement of NRAMP1 from *Arabidopsis thaliana* in iron transport. Biochem. J. **347:** 749–755.

Delhaize, E. (1996). A metal-accumulator mutant of *Arabidopsis thaliana*. Plant Physiol. **111:** 849–855.

Delhaize, E., Gruber, B.D., Pittman, J.K., White, R.G., Leung, H., Miao, Y., Jiang, L., Ryan, P.R., and Richardson, A.E. (2007). A role for the AtMTP11 gene of Arabidopsis in manganese transport and tolerance. Plant J. **51:** 198–210.

Durrett, T.P., Gassmann, W., and Rogers, E.E. (2007). The FRD3-mediated efflux of citrate into the root vasculature is necessary for efficient iron translocation. Plant Physiol. **144:** 197–205.

Eide, D., Broderius, M., Fett, J., and Guerinot, M.L. (1996). A novel iron-regulated metal transporter from plants identified by functional expression in yeast. Proc. Natl. Acad. Sci. USA **93:** 5624–5628.

Eyal, Y., Curie, C., and McCormick, S. (1995). Pollen specificity elements reside in 30 bp of the proximal promoters of two pollen-expressed genes. Plant Cell **7:** 373–384.

Fleming, M.D., Romano, M.A., Su, M.A., Garrick, L.M., Garrick, M.D., and Andrews, N.C. (1998). Nramp2 is mutated in the anemic Belgrade (b) rat: Evidence of a role for Nramp2 in endosomal iron transport. Proc. Natl. Acad. Sci. USA **95:** 1148–1153.

Fleming, M.D., Trenor III, C.C., Su, M.A., Foernzler, D., Beier, D.R., Dietrich, W.F., and Andrews, N.C. (1997). Microcytic anaemia mice have a mutation in Nramp2, a candidate iron transporter gene. Nat. Genet. **16:** 383–386.

Gadd, G.M., and Laurence, O.S. (1996). Demonstration of high-affinity Mn^{2+} uptake in Saccharomyces *cerevisiae*: Specificity and kinetics. Microbiology **142:** 1159–1167.

Gunshin, H., Mackenzie, B., Berger, U.V., Gunshin, Y., Romero, M.F., Boron, W.F., Nussberger, S., Gollan, J.L., and Hediger, M.A. (1997). Cloning and characterization of a mammalian proton-coupled metal-ion transporter. Nature **388:** 482–488.

Hall, J.L., and Williams, L.E. (2003). Transition metal transporters in plants. J. Exp. Bot. **54:** 2601–2613.

Jensen, L.T., Ajua-Alemanji, M., and Culotta, V.C. (2003). The *Saccharomyces cerevisiae* high affinity phosphate transporter encoded by PHO84 also functions in manganese homeostasis. J. Biol. Chem. **278:** 42036–42040.

Jensen, L.T., Carroll, M.C., Hall, M.D., Harvey, C.J., Beese, S.E., and Culotta, V.C. (2009). Down-regulation of a manganese transporter in the face of metal toxicity. Mol. Biol. Cell **20:** 2810–2819.

Kaiser, B.N., Moreau, S., Castelli, J., Thomson, R., Lambert, A., Bogliolo, S., Puppo, A., and Day, D.A. (2003). The soybean NRAMP homologue, GmDMT1, is a symbiotic divalent metal transporter capable of ferrous iron transport. Plant J. **35:** 295–304.

Keen, C.L., Ensunsa, J.L., and Clegg, M.S. (2000). Manganese metabolism in animals and humans including the toxicity of manganese. Met. Ions Biol. Syst. **37:** 89–121.

Kehres, D.G., Zaharik, M.L., Finlay, B.B., and Maguire, M.E. (2000). The NRAMP proteins of *Salmonella typhimurium* and *Escherichia coli* are selective manganese transporters involved in the response to reactive oxygen. Mol. Microbiol. **36:** 1085–1100.

Korshunova, Y.O., Eide, D., Clark, W.G., Guerinot, M.L., and Pakrasi, H.B. (1999). The IRT1 protein from *Arabidopsis thaliana* is a metal transporter with a broad substrate range. Plant Mol. Biol. **40:** 37–44.

Lahner, B., Gong, J., Mahmoudian, M., Smith, E.L., Abid, K.B., Rogers, E.E., Guerinot, M.L., Harper, J.F., Ward, J.M., McIntyre, L., Schroeder, J.I., and Salt, D.E. (2003). Genomic scale profiling of nutrient and trace elements in *Arabidopsis thaliana*. Nat. Biotechnol. **21:** 1215–1221.

Lanquar, V., Lelièvre, F., Barbier-brygoo, H., and Thomine, S. (2004). Regulation and function of AtNRAMP4 metal transporter protein. Soil Sci. Plant Nutr. **50:** 1141–1150.

Lanquar, V., Lelievre, F., Bolte, S., Hames, C., Alcon, C., Neumann, D., Vansuyt, G., Curie, C., Schroder, A., Kramer, U., Barbier-Brygoo, H., and Thomine, S. (2005). Mobilization of vacuolar iron by AtNRAMP3 and AtNRAMP4 is essential for seed germination on low iron. EMBO J. **24:** 4041–4051.

Lasat, M.M., Baker, A., and Kochian, L.V. (1996). Physiological characterization of root Zn^{2+} absorption and translocation to shoots in Zn hyperaccumulator and nonaccumulator species of Thlaspi. Plant Physiol. **112:** 1715–1722.

Li, X., Chanroy, S., Wu, Z., Romanowsky, S.M., Harper, J.F., and Sze, H. (2008). A distinct endosomal Ca^{2+}/Mn^{2+} pump affects root growth through the secretory process. Plant Physiol. **147:** 1675–1689.

Liu, X.F., and Culotta, V.C. (1999). Post-translation control of Nramp metal transport in yeast. Role of metal ions and the BSD2 gene. J. Biol. Chem. **274:** 4863–4868.

Lurin, C., et al. (2004). Genome-wide analysis of *Arabidopsis* pentatricopeptide repeat proteins reveals their essential role in organelle biogenesis. Plant Cell **16:** 2089–2103.

Makui, H., Roig, E., Cole, S.T., Helmann, J.D., Gros, P., and Cellier, M.F. (2000). Identification of the *Escherichia coli* K-12 Nramp orthologue (MntH) as a selective divalent metal ion transporter. Mol. Microbiol. **35:** 1065–1078.

Marschner, H. (1995). Mineral Nutrition of Higher Plants. (London: Academic Press).

Maser, P., et al. (2001). Phylogenetic relationships within cation transporter families of Arabidopsis. Plant Physiol. **126:** 1646–1667.

Merchant, S., and Sawaya, M.R. (2005). The light reactions: A guide to recent acquisitions for the picture gallery. Plant Cell **17:** 648–663.

Mills, R.F., Doherty, M.L., Lopez-Marques, R.L., Weimar, T., Dupree, P., Palmgren, M.G., Pittman, J.K., and Williams, L.E. (2008). ECA3,

a Golgi-localized P2A-type ATPase, plays a crucial role in manganese nutrition in Arabidopsis. Plant Physiol. **146:** 116–128.

Mizuno, T., Usui, K., Horie, K., Nosaka, S., Mizuno, N., and Obata, H. (2005). Cloning of three ZIP/Nramp transporter genes from a Ni hyperaccumulator plant *Thlaspi japonicum* and their Ni^{2+}-transport abilities. Plant Physiol. Biochem. **43:** 793–801.

Nevo, Y., and Nelson, N. (2006). The NRAMP family of metal-ion transporters. Biochim. Biophys. Acta **1763:** 609–620.

Oomen, R.J., Wu, J., Lelievre, F., Blanchet, S., Richaud, P., Barbier-Brygoo, H., Aarts, M.G., and Thomine, S. (2009). Functional characterization of NRAMP3 and NRAMP4 from the metal hyperaccumulator *Thlaspi caerulescens*. New Phytol. **181:** 637–650.

Pedas, P., Hebbern, C.A., Schjoerring, J.K., Holm, P.E., and Husted, S. (2005). Differential capacity for high-affinity manganese uptake contributes to differences between barley genotypes in tolerance to low manganese availability. Plant Physiol. **139:** 1411–1420.

Pedas, P., Ytting, C.K., Fuglsang, A.T., Jahn, T.P., Schjoerring, J.K., and Husted, S. (2008). Manganese efficiency in barley: Identification and characterization of the metal ion transporter HvIRT1. Plant Physiol. **148:** 455–466.

Peiter, E., Montanini, B., Gobert, A., Pedas, P., Husted, S., Maathuis, F.J., Blaudez, D., Chalot, M., and Sanders, D. (2007). A secretory pathway-localized cation diffusion facilitator confers plant manganese tolerance. Proc. Natl. Acad. Sci. USA **104:** 8532–8537.

Pittman, J.K. (2005). Managing the manganese: Molecular mechanisms of manganese transport and homeostasis. New Phytol. **167:** 733–742.

Portnoy, M.E., Liu, X.F., and Culotta, V.C. (2000). *Saccharomyces cerevisiae* expresses three functionally distinct homologues of the nramp family of metal transporters. Mol. Cell. Biol. **20:** 7893–7902.

Rengel, Z. (2000). Manganese uptake and transport in plants. Met. Ions Biol. Syst. **37:** 57–87.

Rogers, E.E., and Guerinot, M.L. (2002). FRD3, a member of the multidrug and toxin efflux family, controls iron deficiency responses in *Arabidopsis*. Plant Cell **14:** 1787–1799.

Supek, F., Supekova, L., Nelson, H., and Nelson, N. (1996). A yeast manganese transporter related to the macrophage protein involved in conferring resistance to mycobacteria. Proc. Natl. Acad. Sci. USA **93:** 5105–5110.

Suzuki, T., Momoi, K., Hosoyamada, M., Kimura, M., and Shibasaki, T. (2008). Normal cadmium uptake in microcytic anemia mk/mk mice suggests that DMT1 is not the only cadmium transporter in vivo. Toxicol. Appl. Pharmacol. **227:** 462–467.

Thomine, S., Wang, R., Ward, J.M., Crawford, N.M., and Schroeder, J.I. (2000). Cadmium and iron transport by members of a plant metal transporter family in Arabidopsis with homology to Nramp genes. Proc. Natl. Acad. Sci. USA **97:** 4991–4996.

Thompson, K., Molina, R.M., Donaghey, T., Schwob, J.E., Brain, J.D., and Wessling-Resnick, M. (2007). Olfactory uptake of manganese requires DMT1 and is enhanced by anemia. FASEB J. **21:** 223–230.

Vert, G., Grotz, N., Dedaldechamp, F., Gaymard, F., Guerinot, M.L., Briat, J.F., and Curie, C. (2002). IRT1, an *Arabidopsis* transporter essential for iron uptake from the soil and for plant growth. Plant Cell **14:** 1223–1233.

Vert, G.A., Briat, J.F., and Curie, C. (2003). Dual regulation of the Arabidopsis high-affinity root iron uptake system by local and long-distance signals. Plant Physiol. **132:** 796–804.

Vidal, S.M., Malo, D., Vogan, K., Skamene, E., and Gros, P. (1993). Natural resistance to infection with intracellular parasites: Isolation of a candidate for Bcg. Cell **73:** 469–485.

Wei, W., Chai, T., Zhang, Y., Han, L., Xu, J., and Guan, Z. (2009). The *Thlaspi caerulescens* NRAMP homologue TcNRAMP3 is capable of divalent cation transport. Mol. Biotechnol. **41:** 15–21.

Xiao, H., Yin, L., Xu, X., Li, T., and Han, Z. (2008). The iron-regulated transporter, MbNRAMP1, isolated from *Malus baccata* is involved in Fe, Mn and Cd trafficking. Ann. Bot. (Lond.) **102:** 881–889.

Yang, T.J., Perry, P.J., Ciani, S., Pandian, S., and Schmidt, W. (2008). Manganese deficiency alters the patterning and development of root hairs in Arabidopsis. J. Exp. Bot. **59:** 3453–3464.

High-Affinity Manganese Uptake by the Metal Transporter NRAMP1 Is Essential for *Arabidopsis* Growth in Low Manganese Conditions

Rémy Cailliatte, Adam Schikora, Jean-François Briat, Stéphane Mari and Catherine Curie

Plant Cell 2010;22;904-917; originally published online March 12, 2010;
DOI 10.1105/tpc.109.073023